Phase-Locked Millimeter-Wave Two-Port Second-Harmonic Gunn Oscillators

Robert G. Davis, Michael J. Leeson, *Student Member, IEEE*, Howard D. G. Lennon, and Max J. Lazarus, *Senior Member, IEEE*

Abstract—**Two-port harmonic oscillators have been developed which are suitable for VCO operation in frequency stabilized systems. For wide-band tunable operation, an oscillator with a varactor-tunable fundamental cavity located vertically above the harmonic cavity has been constructed, and this oscillator has been stabilized in a phase-locked loop. An alternative bias-tuned in-line configuration is also reported which is on a single plane so that an integrated monolithic version is conceivable.**

I. Introduction

PREVIOUS work [1]–[3] has drawn attention to the convenience of using a two-port oscillator so that a portion of the output power can be sampled for AFC or phase locking, without the introduction of additional lossy components. At millimeter-wave frequencies many oscillators use the technique of harmonic extraction from Gunn diodes [4]–[7]. This is a cost-effective method of operation which provides high spectral purity and high stability against frequency pulling [6]. The latter advantage can be very important for phase-lock loop control, since it is essential to prevent the oscillator from being pulled out of the locking range of the loop by adverse loads. Harmonic mode oscillators achieve this stability without the requirement of an isolator because the fundamental circuit is not significantly affected by the external load presented to the harmonic output circuit. Furthermore, since the fundamental oscillations are now at much lower frequencies, electronic tuning using varactors is more cost effective and technically less difficult.

A feature of the present work is that the output sample required for the control circuitry can be taken from the plentiful fundamental power [3]. This maximizes the harmonic power available to the load and reduces the order of harmonic mixing required to generate the control IF. The advantage of this arrangement can be illustrated with the mathematical modeling of the harmonic superheterodyne mixer. For an idealized mixer diode, the conversion conductance for nth-harmonic mixing is proportional to the modified Bessel function $I_n(eV_{LO}/\eta kT)$ [8]. If the fundamental frequency is used at, for example, 33.804 GHz with a 5.616 GHz local oscillator, this would result in an IF of 108 MHz for $n = 6$. However the use of the millimeter-wave harmonic at 67.608 GHz would require $n = 12$. It is a straightforward computational exercise to show that the ratio of the conversion conductances, $I_n(x)/I_{2n}(x)$, will always be large and hence that stabilization of a harmonic-mode oscillator using the fundamental frequency greatly reduces the demands on the performance of the harmonic mixer.

Two oscillator designs are reported in this paper. The first has a fundamental frequency cavity located above the harmonic output cavity and the fundamental is coupled by means of the Gunn device bias-line filter. The second design is an in-line structure which uses a waveguide taper as the filter element separating the fundamental and harmonic frequency components. The latter design is a translation of the first oscillator concept onto a single plane, so that the prospect of an integratable version can be readily envisaged.

II. Varactor-Tuned Twin-Cavity Oscillator

A. The Oscillator Circuit

The first oscillator described is shown in Fig. 1 and consists of a two-cavity structure with an output port from each cavity. The lower port delivers the main output, which is at the second harmonic frequency. The subsidiary port is located above and orthogonal to the harmonic cavity, and provides the reference output at the fundamental frequency. The primary oscillation is provided by a Gunn device[1] and a cap resonator located in the lower waveguide. The oscillation has a fundamental frequency of ~35 GHz and produces a second-harmonic output of ~70 GHz. The lower waveguide delivers the harmonic frequency and this output power is optimized by the use of an adjustable back-short. Maximum power is achieved for a back-short position of approximately $3\lambda_g/4$ from the center of the cap (the cap diameter preventing

Manuscript received March 1, 1990; revised April 24, 1991. This work was supported by the Science and Research Council of the U.K. under Grant GR/D 64513.

R. G. Davis was with the Department of Physics, University of Lancaster, Lancaster, England. He is now with the DRA Electronics Division, RSRE Malvern, St Andrews Rd, Malvern, WR14 3PS, England.

M. J. Leeson was with the Department of Physics, University of Lancaster, Lancaster, England. He is now with the Department of Physics, University of St Andrews, St Andrews, KY16 9SS, Scotland, U.K.

H D. G. Lennon and M. J. Lazarus are with the Department of Physics, University of Lancaster, Lancaster, LA1 4YB, England.

IEEE Log Number 9102330.

[1]Type DGB8556-89, Alpha Industries, Woburn, MA (package style 296).

0018-9480/91/1000-1746$01.00 ©1991 IEEE

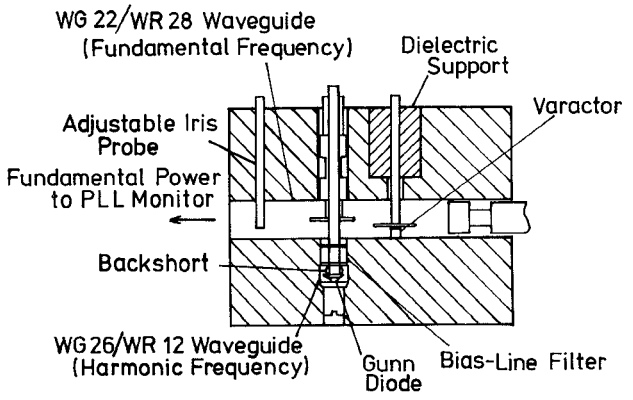

Fig. 1. Schematic diagram of the twin-cavity oscillator.

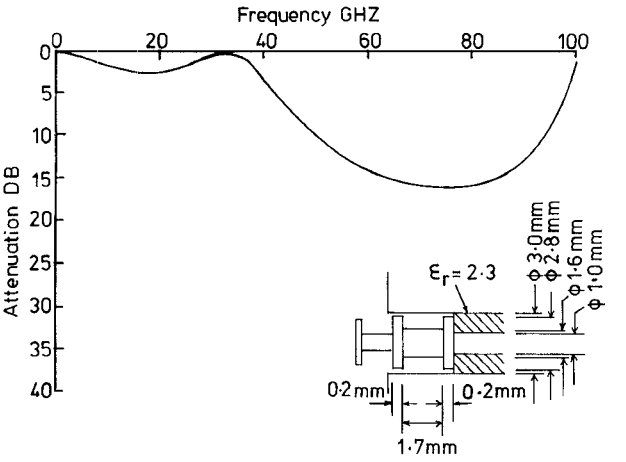

Fig. 2. Calculated performance of the bias-line filter.

the use of the $\lambda_g/4$ position). The fundamental frequency is below the cutoff frequency of this waveguide and so it is confined, as in the conventional harmonic oscillator. The upper tuning cavity is constructed from larger waveguide which supports the propagation of the fundamental frequency. This cavity is coupled to the primary oscillation by a short coaxial filter which is formed by the Gunn device bias line and its surrounding channel [3], [9]. The cavity is tuned either mechanically, using a tunable short circuit, or electrically with a varactor diode arrangement. The fundamental frequency output of the oscillator is sampled by the iris structure to the left of Fig. 1 and is restricted to a small fraction of the available power. This output provides the monitor signal for the stabilizing system. The use of the two-port oscillator concept is demonstrated, successfully stabilizing the oscillation with a phase-locked loop arrangement. For alternative operation as a single-port oscillator, the probe can be replaced by a short circuit so that the cavity is totally enclosed.

B. The Coupling Filter

The fundamental-frequency cavity is coupled to the diode resonator by means of a low-pass coaxial filter followed by a second cap structure which forms a radial line transformer to match the low-impedance coaxial line to the high-impedance fundamental-frequency waveguide. The bias-line filter is crucial to the operation of the oscillator. The coupling of the fundamental power into the tuning cavity must be maximized to obtain the best tuning range, while the harmonic power should see a reflecting short circuit in order to optimize the output power at this frequency. It is to be expected that the fundamental power in the harmonic waveguide will couple well to the coaxial line because this frequency is beyond the cutoff frequency of the waveguide and will be in a coaxial type mode around the cap assembly.

The filter structure is constructed from two thin disks separated by a distance of $\lambda_f/4$, where λ_f is the wavelength of the fundamental frequency. At this frequency, the large susceptance produced by the first disk will be tuned out by the transformed susceptance of the second one, and so the structure will pass the fundamental with low attenuation. However, at the harmonic frequency the spacing is $\lambda/2$ and so the susceptance of the first disk is reinforced by that of the second, thus presenting a short circuit. The detailed design of the filter was determined by theoretical modeling. A computer program was developed which calculates its attenuation as a function of frequency, once a few assumptions regarding the source and load impedances have been made [10]. The assumptions are:

i) The cap at the top of the bias line matches the characteristic impedance of the last section of the coaxial filter to that of the upper waveguide.
ii) The source impedance of the filter is that of a quasi-coaxial mode propagation produced around the stem of the resonant cap located on top of the Gunn device.

The program calculates the A matrix of each coaxial line element and cascades them together with suitable discontinuity capacitances [11] to determine the overall matrix for the whole assembly. The attenuation characteristic is then readily calculated from this overall matrix using the expressions derived in [11]. The initial estimate of the filter dimensions are then optimized until the desired characteristic is obtained. The dimensions used, together with the predicted attenuation characteristic, are given in Fig. 2. The figure shows a dielectric spacer placed behind the filter to position it correctly in the channel.

C. Varactor Tuning

The varactor is coupled to the upper cavity by means of a third cap structure and an adjustable back-short. Fig. 3 shows measurements of the reflection coefficient presented by the varactor assembly. The measurements are given relative to the reference plane located at the center of the varactor package. The solid curve shows the impedance as the back-short is varied. This rotates from a short circuit (point 1), where the back-short is a half a wavelength from the center of the varactor, to the point

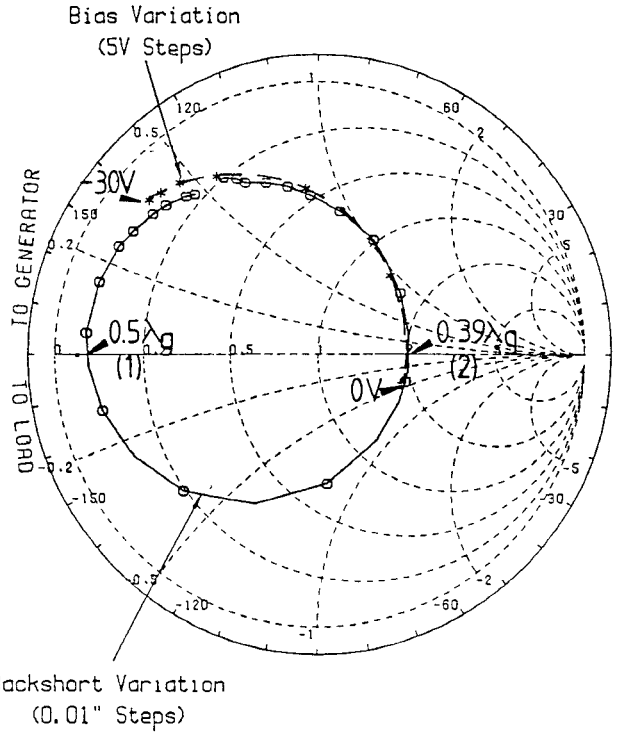

Fig. 3. Measurement of the reflection coefficient presented by the varactor assembly (varactor A).

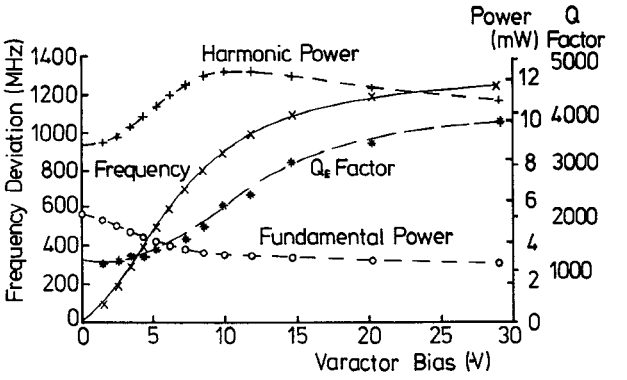

Fig. 4. Twin-cavity oscillator tuning performance (varactor A).

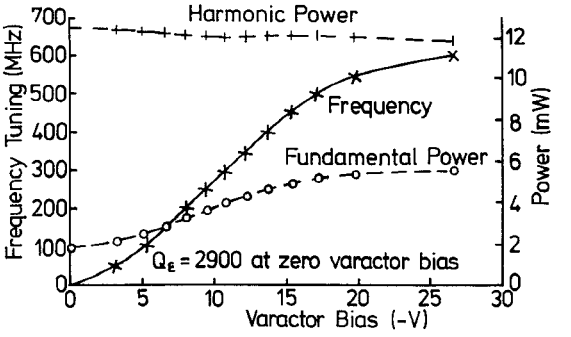

Fig. 5. Twin-cavity oscillator tuning performance (varactor B).

of maximum coupling (point 2, at 0.39 wavelengths), where the susceptance of the varactor assembly is canceled by an equal and opposite susceptance provided by a suitable back-short offset. The dashed curve shows the effect of changing the bias from the point of optimal coupling. The oscillator tuning mechanism can be understood by realizing that the bias dependence of the reflection coefficient phase modifies the effective length of the upper cavity and hence its resonant frequency. The oscillation frequency is pulled an amount dependent on the cavity resonant frequency and on its coupling to the primary resonator in the harmonic waveguide. For the maximum tuning range, the variation in reflection coefficient angle must be maximized; however the magnitude of the reflection coefficient is also important as this largely determines the loss in the cavity. Tuning range and loss are observed to occur at the expense of each other and a compromise is necessary. Measurements showed that a varactor[2] with a zero bias capacitance, C_{j0}, of about 1 pF gives a reasonable compromise between the minimum magnitude of reflection coefficient and the change in angle over the bias range. The varactor cap diameter is required to be a significant fraction of a wavelength to produce an effective radial transformer. Reliable transformer operation is obtained for a cap diameter greater than 3 mm, and excellent results are obtained for a diameter of 4 mm [10].

[2]Device type MA46570E, Microwave Associates, Dunstable, Beds., England.

The varactor is located at a nominal half wavelength from the low-impedance coupling post and cap assembly. The exact position is not critical owing to the transformer action of the caps. The coupling of the upper tuning cavity to the main oscillator circuit is optimized by observing the magnitude of the shift in output frequency with varactor back-short movement. The cavity is strongly coupled when the effect on the frequency is large. Fine adjustment of the optimum coupling point is achieved by using the varactor as a detector diode and adjusting the varactor back-short to a position where the rectified voltage is a maximum. The harmonic output power can be increased at the expense of the tuning range by decoupling the varactor circuit slightly. The fraction of the fundamental power which is released to form the second output is controlled by the adjustable probe mismatch.

D. Oscillator Performance

An example of the oscillator performance is given in Fig. 4. The oscillator achieves a tuning range of 1200 MHz with a power variation of 1.5 dB, for a zero tuning bias frequency of 72 GHz and output power of 10 dBm. The external Q factor (Q_E) is measured by frequency pulling and is seen to increase across the tuning range as the loss in the varactor decreases. The varactor used to obtain these results (varactor A) is specified to have a capacitance of $C_{j-2} = 0.81$ pF for a -2 V bias and a capacitance ratio $C_{j-2}/C_{j-20} = 3.1$. Fig. 5 shows the

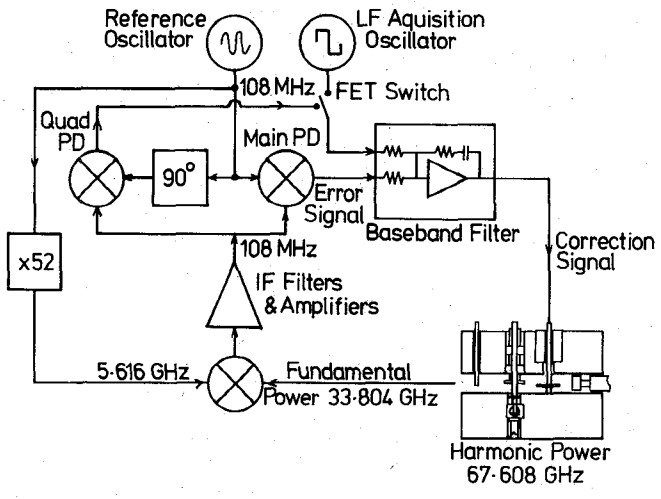

Fig. 6. Heterodyne phase-locked loop stabilization system.

performance with a varactor of larger capacitance (varactor B). Here $C_{j-2} = 1.96$ pF and $C_{j-2}/C_{j-20} = 6.1$. A smaller tuning range of 600 MHz is obtained with a greatly reduced power variation. An important factor in determining the effectiveness of the oscillator design is the extent to which the tuning mechanism limits the output power available from the device. The Gunn diodes used in these experiments produced 15 mW at 70 GHz when operated in a conventional harmonic oscillator structure with no external tuning cavity. The results of Figs. 4 and 5 show the oscillator design to be very economical in the trade-off of output power for tuning range.

E. Phase-Locking the Oscillator

The oscillator is phase-locked using the system of Fig. 6. The figure shows the schematic of the heterodyne loop used. Quadrature phase detectors allow lock to be detected so that the acquisition oscillator can be turned off once the system is locked. The loop filter is an operational amplifier integrator. This circuit has summing inputs so that the step input from the acquisition oscillator is integrated to form a ramp which sweeps the output frequency until lock is achieved [2]. The frequency multiplication required for the harmonic mixer drive is provided by a $\times 52$ phase-locked multiplier. The natural frequency, f_n, of the loop is 130 kHz and is measured using the technique of modulating the VCO [12].

The free running and phase-locked spectra are shown in Fig. 7 (the photograph of the free running spectrum being broadened by low frequency jitter.) The locked oscillator phase noise spectrum in a 1 Hz bandwidth is approximately determined from a spectrum analyzer display and is better than -65 dBc at 1 kHz offset and -100 dBc at 130 kHz offset. The loop is observed to remain locked for all load impedances by fitting a tunable short circuit on the harmonic frequency output port and tuning it over all phases. This feature is important if the oscillator is to feed a nonideal load such as an antenna

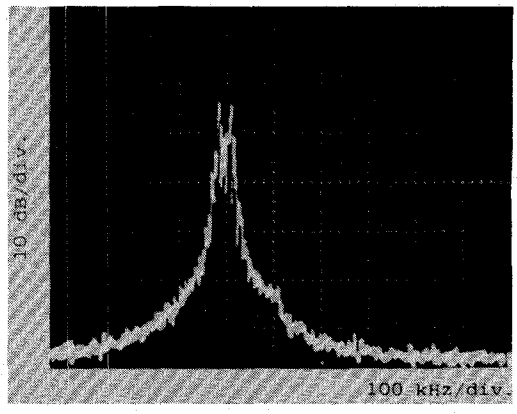

(a)

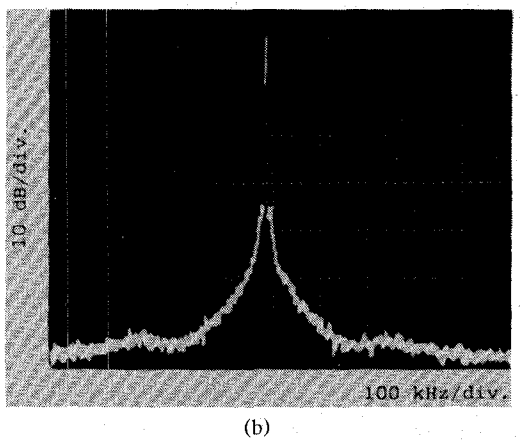

(b)

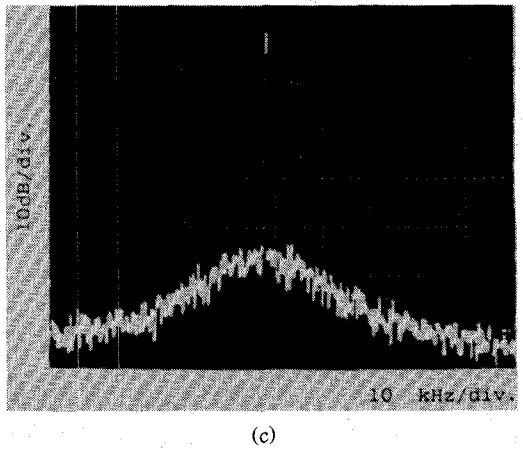

(c)

Fig. 7. Free running and phase-locked spectra of the twin-cavity oscillator: (a) Free running; (b) phase-locked; (c) phase-locked.

where the reflections from nearby objects can pull the oscillator frequency. In order for the loop to remain locked, the pulling range of the oscillator should be much less than the range in which the loop can retune it. This condition is easily satisfied by the high Q of the present system. The total deviation of the unlocked fundamental frequency for a short circuit harmonic load, tuned over all phases, is ~ 20 MHz. The corresponding Q_E factor for the harmonic circuit measured at the loop operating point was found to be approximately 3400.

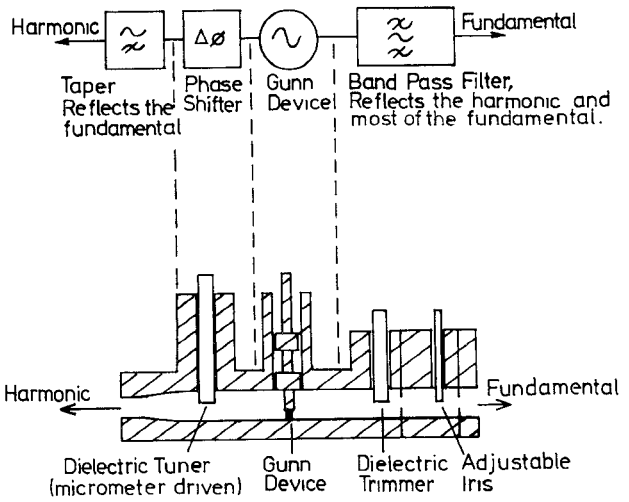

Fig. 8. Philosophy and schematic diagram of the tapered waveguide oscillator.

III. Bias-Tuned Tapered Waveguide Oscillator

A. The Oscillator Circuit

The second oscillator presented is a translation into an in-line geometry of the ideas discussed for the first structure. A high-pass filter can be constructed using tapered waveguide which is chosen to be beyond cutoff for the fundamental frequency. This structure can be designed to transmit the harmonic in the TE_{10} mode while giving nearly perfect reflection of the fundamental. The cutoff acts as an almost ideal open circuit, since the waveguide impedance has a pole at this frequency. The oscillator is shown in Fig. 8. The fundamental resonant length between the Gunn device and taper reflection is tuned by means of a micrometer-driven dielectric phase-shifter insert which can be calibrated. The high-pass taper has a cutoff frequency just below 50 GHz. In these experiments the fundamental frequencies were in the range 35.5–36.1 GHz, giving a 71–72.2 GHz harmonic output). The low-pass filter consists of a tunable cavity, formed by two irises on either side of a metal tuning piston. It was found that improved harmonic performance could be obtained by means of a rexolite trimmer located between the iris cavity and the Gunn diode. The theory for the resonance between the taper and the Gunn diode, and its tuning with the dielectric phase-shifter, is presented in the following subsections.

B. Resonant Lengths of Tapered Waveguides for Diode Oscillators

In the conventional post-coupled diode oscillator, the resonator is a length of straight waveguide terminated with a back-short. The resonant length is usually $\sim \lambda_g/2$ or $m\lambda_g/2$, where m is an integer, since the diode usually oscillates near a minimum impedance of the standing wave. For the tapered waveguide replacing the back-short, the cutoff point behaves like an open circuit and so the resonance will correspond to $(m+1/2)$ times the half wavelength, with the complication that $\lambda_g/2$ is now no longer the constant of a straight waveguide. This type of problem, i.e., of a wave in which the spatial phase factor is not a constant (like $\beta = 2\pi/\lambda$) but is itself a function of position, has been extensively studied in the analogous case of quantum mechanics [13]. Fortunately, the complexities of the additional differential equations arising from the complete W.K.B. (Wentzel–Kramers–Brillouin) analysis can be avoided for the following reasons. First, the tapers used have only a gradual width variation, since they are required to transmit the harmonic. Second, only the maxima and minima which arise from superposition of functions of the form $e^{\pm j\int\beta\,dz}$ are of interest, and for the case of these representing incident and reflected waves in a loss-free tapered guide, the amplitudes will be the same at a given point. A convenient coordinate system for this is shown in Fig. 9. With the above considerations the tapered waveguide field is assumed to be a small perturbation on the functions for the straight guide. Thus the TE_{10} fields have their time and z dependences as $e^{j(\omega t \pm \int\beta\,dz)}$ while the other familiar conditions assume the usual form from Maxwell's equations:

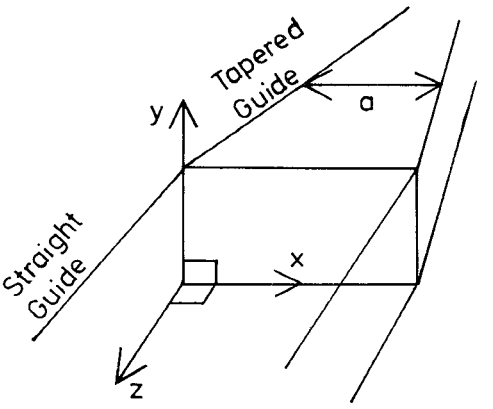

Fig. 9. The tapered waveguide oscillator coordinate system.

$$E_x = 0 \qquad E_z = 0 \qquad \frac{\partial}{\partial y} = 0,$$

$$E_y \propto \sin\frac{\pi x}{a} \qquad H_x \propto E_y.$$

Variation of the height in the y direction affects only the impedance. With the assumption of gradual variation of taper width, the wave equation:

$$\frac{\partial^2 E_y}{\partial x^2} + \frac{\partial^2 E_y}{\partial z^2} = \frac{1}{c^2}\frac{\partial^2 E_y}{\partial t^2} \tag{1}$$

then yields the solutions of the form $E_y \propto e^{\pm j\int\beta\,dz}$, where

$$\beta = \left[\frac{\omega^2}{c^2} - \frac{\pi^2}{a^2}\right]^{1/2} \tag{2}$$

and a is a function of position, z. The quasi-infinite impedance of the taper at cutoff is such that the current and magnetic field are virtually zero while the voltage and

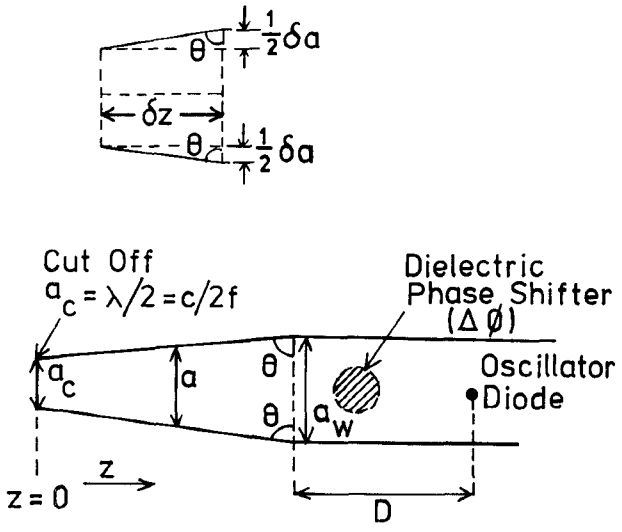

Fig. 10. Geometry and parameters for the tapered waveguide oscillator resonance analysis.

electric field are at a maximum given by the superposition: $E_{\text{incident}} + E_{\text{reflected}}$. Thus the electric field is of the form

$$E = A(z)e^{j(\omega t + \int_0^z \beta\, dz)} + A(z)e^{j(\omega t - \int_0^z \beta\, dz)}. \quad (3)$$

For the loss-free case, the amplitudes $A(z)$ at a given point z will be the same for the incident and reflected waves, yielding the resultant standing wave:

$$E \propto e^{j\omega t} \cdot \cos\left(\int_0^z \beta\, dz\right). \quad (4)$$

For the oscillator diode to be at a minimum impedance at position z in the standing wave pattern then

$$\int_0^z \beta\, dz = \left(m + \frac{1}{2}\right)\pi, \qquad m = 0,1,2,3,\cdots. \quad (5)$$

Referring to Fig. 10 for the geometry, it is seen that the above integral covers the range from $z = 0$ to the diode. The phase shifter changes the electrical path length, thus giving a phase shift component $\Delta\phi$. Together with the nontapered portion of the guide, this gives the phase contribution:

$$\Delta\phi + \left(\frac{\omega^2}{c^2} - \frac{\pi^2}{a_w^2}\right)^{1/2} \cdot D = \Delta\phi + \text{HD}. \quad (6)$$

For the taper itself, a convenient change in the variable is z to a, where $\dfrac{\partial z}{\partial a} = (1/2)\tan\theta$. Equation (5) can now be rewritten as

$$\int_0^z \beta\, dz = \left(\int_{a_c}^{a_w} \beta \frac{dz}{da}\, da\right) + \text{HD} + \Delta\phi$$

$$= \left(\frac{1}{2}\tan\theta \int_{a_c}^{a_w} \beta\, da\right) + \text{HD} + \Delta\phi = \left(m + \frac{1}{2}\right)\pi. \quad (7)$$

The solution of the integral requires substitution for β from (2) and then the substitution $\cos G = \pi c/a\omega$, or $a = (\pi c/\omega)\sec G$ so that $da = (\pi c/\omega)\sec G \tan G\, dG$. With the above changes of variables, (7) becomes

$$\frac{\pi}{2}\tan\theta \int_{G_c}^{G_w} \tan^2 G\, dG + \text{HD} + \Delta\phi = \left(m + \frac{1}{2}\right)\pi \quad (8)$$

where

$$G_w = \arccos\frac{\pi c}{a_w \omega} \qquad G_c = \arccos\frac{\pi c}{a_c \omega} = 0. \quad (9)$$

Now since

$$\int_0^{G_w} \tan^2 G\, dG = \tan G_w - G_w \quad (10)$$

then (8) finally becomes

$$\frac{\pi}{2}\tan\theta(\tan G_w - G_w) + \text{HD} + \Delta\phi - \left(m + \frac{1}{2}\right)\pi = 0 \quad (11)$$

with

$$G_w = \arccos\frac{\pi c}{a_w \omega} \qquad H = \left[\frac{\omega^2}{c^2} - \frac{\pi^2}{a_w^2}\right]^{1/2}.$$

Equation (11) thus relates the resonant frequency, $\omega/2\pi$, of the taper section to the waveguide and taper dimensions and the additional phase shift $\Delta\phi$. The solution frequencies are given by the roots of this implicit transcendental equation, which are calculated using a library subroutine.[3]

C. Practical Implementation of the Tapered Waveguide Oscillator

A compact phase shifting tuner in the form of the dielectric rod allows the integer m of (11) to be kept reasonably small. For these experiments, this assembly is micrometer driven and is calibrated using a standing wave indicator. For a diode operating in the fundamental band from 35.5 to 36.1 GHz, the taper dimensions used are

$$D = 2.41 \text{ mm}$$
$$a_w = 7.0 \text{ mm}$$
$$\theta = 1.516 \text{ rad}.$$

These data are used in (11) to calculate the solution frequencies of the taper resonance. A comparison between experiment and theory is shown in Fig. 11. The results confirm that, for our practical convenient mode number of $m = 8$, the mode is sufficiently well separated from the adjacent modes to preclude mode jumping. The low-pass iris structure is a waveguide analogue of the coaxial filter of the varactor-tuned oscillator. The response for the overmoded harmonic is less predictable, but the empirically tuned results are satisfactory. The iris assembly is placed sufficiently far from the Gunn diode to avoid heating effects and the position of the first iris should not be at $n\lambda_g/2$, to prevent spurious resonance.

[3]Subroutine C05ADF of the NAG FORTRAN library. Numerical Algorithms Group Ltd, Mayfied House, 256 Banbury Road, Oxford, OX2 7DE, England.

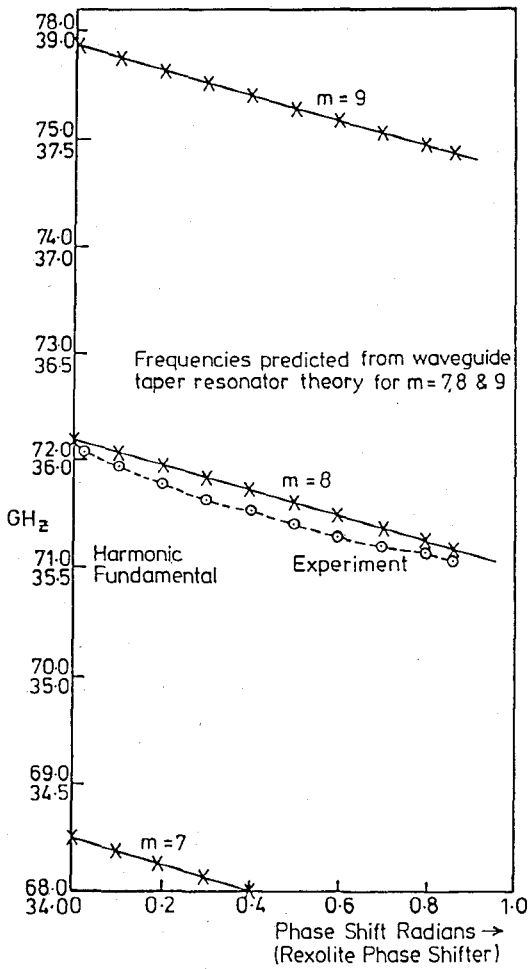

Fig. 11. Mode chart for the tapered waveguide oscillator.

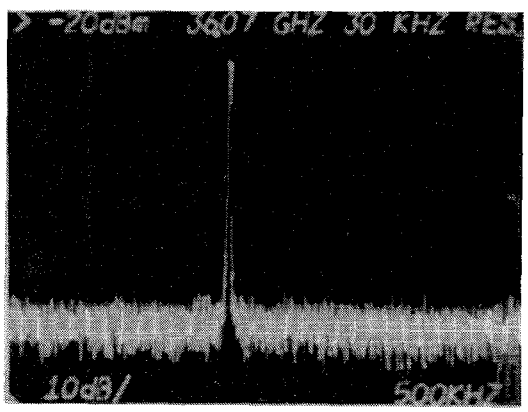

Fig. 12. Spectral performance of the tapered waveguide oscillator (fundamental output).

The fundamental and harmonic power optima are adjusted with the dielectric trimmer or the metal piston in the iris cavity. The oscillator delivers output powers up to 15 mW in the 71–72 GHz band with several tens of milliwatts in the 35.5–36 GHz band. The spectrum obtained is shown in Fig. 12. No observable frequency pulling is detected on the introduction of a mismatch to the harmonic waveguide output. The electronic tuning of the taper oscillator will of course vary from diode to diode, but it is generally at least 10 kHz per millivolt with bias tuning, which is adequate for phase-locking. However, if varactor tuning is required, then a suitable arrangement could be designed in a manner similar to the tuning cavity of the first oscillator structure.

IV. Conclusion

Electronically tunable two-port second-harmonic Gunn oscillator structures have been developed. The oscillators have output ports for both the fundamental and harmonic frequencies and are suitable for cost-effective frequency stabilization systems. The oscillator designs and performance have been discussed and a demonstration of their use in a heterodyne phase-locked loop control system has been presented.

The techniques necessary for the realization of integrated oscillator structures are now reaching maturity [14]–[18]. The second oscillator structure reported in this work is directly transferrable to dielectric, metallized dielectric, and metallized plastic injection molded waveguide media. The use of microstrip for dielectric resonator oscillators will require the design of suitable microstrip filter structures in order to isolate the fundamental and harmonic frequency components.

Acknowledgment

The authors would like to acknowledge Dr. R. N. Bates of Philips Research Laboratories, Redhill, Surrey, for helpful discussions and to thank I. Matthews and J. Heseltine for their help in preparing this manuscript.

References

[1] M. J. Lazarus and R. G. Davis, "A two-port millimeter-wave oscillator," *Microwave J.*, vol. 28, pp. 165–170, Mar. 1985.

[2] R. G. Davis and M. J. Lazarus, "Phase locking of mm-wave two-port Gunn oscillator by bias tuning," *Microwave J.*, vol. 29, pp. 103–107, June 1986.

[3] R. G. Davis and M. J. Lazarus, "A varactor tuned millimeter wave two-port harmonic Gunn oscillator suitable for phase locking, in *Dig. I.E.E. Colloq. Millimetric Wave Component Design* (London), Nov. 1986, pp. 10/1–10/4.

[4] H. Barth, "A wideband, backshort-tunable second harmonic W-band Gunn-oscillator, in *IEEE-MTT-S Int. Microwave Symp. Dig.*, 1981, pp. 334–337.

[5] M. J. Lazarus *et al.*, "Wideband tunable mm-wave Gunn oscillator design," *Electron. Lett.*, vol. 17, no. 20, pp. 739–741, Oct. 1981.

[6] K. Solbach *et al.*, "Harmonic Gunn oscillators allow frequency growth," *Microwaves & RF*, pp. 75 et seq., Apr. 1983.

[7] W. H. Haydl, "Fundamental and harmonic operation of millimeter-wave Gunn diodes," *IEEE Trans. Microwave Theory Tech.*, vol. MTT-31, pp. 879–889, Nov. 1983.

[8] F. A. Benson, *Millimetre and Submillimetre Waves*. London: Iliffe, 1969, ch. 22, p. 470, eq. 51.

[9] K. Jacobs and B. Vowinkel, "Solid state mm-wave oscillators with large tuning range," in *IEEE-MTT-S Int. Microwave Symp. Dig.*, 1987, pp. 863–866.

[10] R. G. Davis, Ph.D. thesis, University of Lancaster, Library, Lancaster, LA1 4YW, England, May 1987.

[11] G. L. Matthai, L. Young and E. M. T. Jones, *Microwave Filters, Impedance Matching Networks and Coupling Structures*. New York: McGraw-Hill, 1964, pp. 38–39 and pp. 203–206.
[12] F. M. Gardner, *Phaselock Techniques*, 1st ed. New York: Wiley, 1966, pp. 124–128.
[13] L. I. Schiff, *Quantum Mechanics*. New York: McGraw-Hill, 1955, p. 186, Eq. 28-7.
[14] H. Jacobs and S. Dixon, Jr., "Millimetre-wave InP image line self mixing Gunn oscillator, *IEEE Trans. Microwave Theory Tech.*, vol. MTT-29, pp. 958–961, Sept. 1981.
[15] M. J. Lazarus, F. R. Pantoja, and M. G. Somekh, "Metallized dielectric horn and waveguide structures for millimeter wave oscillator/mixer systems," *IEEE Trans. Microwave Theory Tech.*, vol. MTT-29, pp. 102–106, Feb. 1981.
[16] P. Mallinson and A. G. Stove, "Car obstacle avoidance radar at 94 GHz," Philips Research Laboratories Annual Review, Redhill, England, 1989, pp. 61–64.
[17] D. C. Smith and T. J. Simmons, "Fully integrated W-band microstrip oscillator," *Electron. Lett.*, vol. 19, no. 6, pp. 222–223, 17 Mar. 1983.
[18] G. B. Morgan, "Dielectric resonators for circuits at short mm wavelengths," *Microwave J.*, pp. 107–115, July 1986.

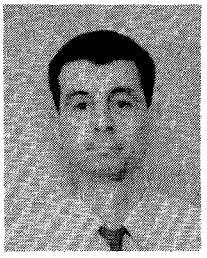

Robert G. Davis graduated in applied physics and electronics in 1983 and received the Ph.D. degree in 1987, both from the University of Lancaster, England.

In 1986, he joined the Royal Signals and Radar Establishment, Malvern, England. His current research activities include microwave device design and nonlinear CAD.

Michael J. Leeson (S'90) was born in Reading, U.K., on June 19, 1966. He received the B. Sc. (Hons) degree in applied physics from Lancaster University, U.K., in 1987.

From 1987 to 1989 he was a research engineer at Smiths Industries Aerospace and Defence Systems, Cheltenham, U.K. He is currently pursuing the Ph.D. degree in the Department of Physics and Astronomy at the University of St. Andrews, Scotland, U.K. His current research interests include quasi-optical techniques and their application to millimeter wave radar.

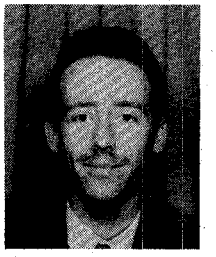

Howard D. G. Lennon was born in Carlisle, U.K., in 1966. He graduated in applied physics and electronics from Lancaster University in 1988. From 1988 to 1989 he was with the Electromagnetic Radiation Department of British Aerospace. Since August 1989 he has been a computer programmer with Stirling Withrop Group, Ltd.

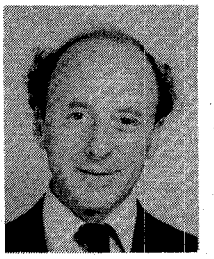

Max J. Lazarus (M'71–SM'83) received the bachelor of science degree in physics from the University of St. Andrews, Scotland, in 1961 and a Doctor of Philosophy degree from Oxford University in 1965.

From 1966 to 1968 he was a lecturer in the Department of Engineering Science at the University of Exeter, England, and in 1968 he took up a lectureship in the Department of Physics at the University of Lancaster. During the period 1974–1975 he was a Visiting Associate Professor at the University of California. He is presently conducting research in millimeter waves, quasi-optical antenna systems, and power transistor electronics.